



Constraining the mass-dependent Ti isotope composition of the chondritic reservoir – An inter-laboratory comparison study

Journal Article

Author(s):

Anguelova, Merislava; Vilela, Nicolas; Kommescher, Sebastian; Greber, Nicolas D.; [Fehr, Manuela](#) ; [Schönbächler, Maria](#) 

Publication date:

2024-05-01

Permanent link:

<https://doi.org/https://doi.org/10.3929/ethz-b-000672342>

Rights / license:

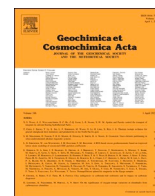
[Creative Commons Attribution 4.0 International](#)

Originally published in:

Geochimica et Cosmochimica Acta 372, <https://doi.org/10.1016/j.gca.2024.01.026>

Funding acknowledgement:

- Tracking planet formation, differentiation and the moon-forming giant impact: an integrated approach using non-traditional stable isotopes ()



Constraining the mass-dependent Ti isotope composition of the chondritic reservoir – An inter-laboratory comparison study

Merislava Anguelova^{a,*}, Nicolas Vilela^b, Sebastian Kommescher^c, Nicolas D. Greber^{b,d},
Manuela A. Fehr^a, Maria Schönbächler^a

^a Institute of Geochemistry and Petrology, ETH Zurich, 8092 Zurich, Switzerland

^b Institute of Geological Sciences, University of Bern, 3012 Bern, Switzerland

^c Institut für Geologie, Mineralogie und Geophysik, Ruhr-Universität Bochum, 44801 Bochum, Germany

^d Muséum d'histoire naturelle de Genève, 1208 Genève, Switzerland

ARTICLE INFO

Associate editor: Helen Williams

Keywords:

Titanium isotopes
Mass-dependent isotope fractionation
Chondritic reservoir
Bulk silicate Earth
Inter-laboratory comparison

ABSTRACT

Titanium isotopes are a promising tracer for planetary differentiation processes. The application of this tracer is, however, currently hampered by the lack of a robust estimate for the chondritic reservoir. Here, we conducted an inter-comparison Ti isotope study of three laboratories with the aim of providing an accurate and precise estimate for the chondritic reservoir. While previous estimates may suffer from heterogeneities on the sampling scale, we chose ordinary chondrites to minimise uncertainties associated with the necessary corrections for nucleosynthetic isotope variations in chondrites, and to allow the analysis of sufficiently large sample sizes representative for bulk meteorites. Titanium isotope data reported by the different laboratories are in good agreement with each other. Ordinary chondrites of different subgroups (H, L, LL) and petrologic types (3–6) display identical Ti isotope compositions within uncertainties (average $\delta^{49}\text{Ti} = +0.023 \pm 0.009\text{‰}$, 2SE, $n = 20$; permille deviation of $^{49}\text{Ti}/^{47}\text{Ti}$ from the OL-Ti standard). The average Ti isotope composition of ordinary chondrites is within 2SE identical to that of OIBs ($+0.029 \pm 0.005\text{‰}$, 2SE, $n = 52$) and all pre 2.7 Ga mafic and komatiitic rocks ($+0.019 \pm 0.006\text{‰}$, 2SE, $n = 58$), indicating that the $\delta^{49}\text{Ti}$ values of the bulk silicate Earth and ordinary chondrites are indistinguishable. Furthermore, our average Ti isotope composition of ordinary chondrites overlaps with those of the Moon, Mars and Vesta, suggesting a homogeneous inner Solar System in terms of mass-dependent Ti isotopes.

1. Introduction

Chondrites contain some of the most primitive materials in the Solar System and represent fragments of undifferentiated parent bodies. They show compositional variability, but because their composition generally resembles the non-volatile portion of the solar photosphere, chondritic meteorites are considered as potential building blocks of rocky planets. The chemical and isotopic composition of chondrites, therefore, provides a crucial baseline for constraining the formation and composition of planetary reservoirs.

Mass-dependent Ti isotopes represent a promising tracer for planetary silicate differentiation (e.g. Greber et al., 2017a; Millet et al., 2016) and continental crust extraction (Deng et al., 2023). Titanium isotopes undergo significant mass-dependent fractionation during magma evolution, producing permille-level Ti isotope variations (expressed as

$\delta^{49}\text{Ti}$, the permille deviation of $^{49}\text{Ti}/^{47}\text{Ti}$ from the OL-Ti standard) observable in volcanic and plutonic rocks (e.g. Aarons et al., 2020; Deng et al., 2019; Greber et al., 2021; Hoare et al., 2020; Millet et al., 2016; Zhao et al., 2020), magmatic cumulates (Storck et al., 2023), and as small-scale heterogeneities in the upper mantle (Anguelova et al., 2022). Moreover, the magnitude of Ti isotope fractionation may strongly depend on the prevailing redox conditions (Deng et al., 2020; Hoare et al., 2020; Rzehak et al., 2021, 2022). This holds particularly true for extraterrestrial materials that formed under reducing conditions (Greber et al., 2017b; Leitzke et al., 2018; Rzehak et al., 2021, 2022; Wang et al., 2020; Williams et al., 2021), where Ti occurs in two oxidation states (Ti^{3+} , Ti^{4+} ; Simon et al., 2016; Sutton et al., 2017). The potential of Ti isotopes to understand and quantify planetary differentiation processes is, however, hampered by the lack of a robust estimate for the chondritic reservoir. Previous studies revealed no significant mass-dependent Ti

* Corresponding author.

E-mail address: m.anguelova@mailbox.org (M. Anguelova).

<https://doi.org/10.1016/j.gca.2024.01.026>

Received 1 July 2023; Accepted 24 January 2024

Available online 1 February 2024

0016-7037/© 2024 The Author(s). Published by Elsevier Ltd. This is an open access article under the CC BY license (<http://creativecommons.org/licenses/by/4.0/>).

isotope variations between major chondrite classes (i.e. carbonaceous, ordinary, enstatite, and Rumuruti chondrites) (Deng et al., 2018b; Deng et al., 2023; Greber et al., 2017b; Williams et al., 2021). Yet, reported $\delta^{49}\text{Ti}$ averages of bulk chondrites systematically differ, ranging from $+0.007 \pm 0.010 \text{ ‰}$ (2SE, $n = 15$; Greber et al., 2017b), closely matching the estimate for the bulk silicate Earth (BSE; Millet et al., 2016), to $+0.071 \pm 0.018 \text{ ‰}$ (2SE, $n = 22$; Deng et al., 2018b). This inter-laboratory $\delta^{49}\text{Ti}$ difference of up to 0.064 ‰ is beyond the 2SD reproducibility of most geochemical reference materials of around $\pm 0.03 \text{ ‰}$ and may result from sample heterogeneity, or analytical artefacts related to sample processing and analysis. For geochemical reference materials, however, Ti isotope data from different labs and different groups are in good agreement within uncertainties. Due to the limited amount of sample material available, meteorite analyses are particularly prone to sampling bias. The $\delta^{49}\text{Ti}$ data of bulk chondrites may be affected by intra-sample heterogeneities in both (i) nucleosynthetic isotope variations (i.e. non-mass-dependent deviations from terrestrial Ti isotope abundances) and (ii) the mass-dependent Ti isotope composition. For instance, Deng et al. (2018b) observed $\delta^{49}\text{Ti}$ variations of more than 0.100 ‰ and an overall poor reproducibility for multiple replicate digestions for carbonaceous chondrites. This scatter was ascribed to the non-representative sampling of isotopically anomalous phases like calcium-aluminium rich inclusions (CAIs), which are abundant in CO- and CV-type chondrites, and resulting invalid corrections for nucleosynthetic variations (Deng et al., 2018b; Williams et al., 2021). Note that the accurate determination of mass-dependent Ti isotope variations in carbonaceous chondrites essentially requires to obtain mass-independent Ti isotope data from the same sample aliquot. This is because $\delta^{49}\text{Ti}$ data are determined by the double spike method (e.g. Siebert et al., 2001), which assumes that a sample and reference standard are related by mass-dependent isotope fractionation only. Nonetheless, this dual approach was only followed by Williams et al. (2021), whereas other authors used data from the literature or made estimates based on ^{50}Ti analyses (Deng et al., 2023). Grain coarsening associated with thermal metamorphism, and inter-mineral Ti isotope fractionation may bias the bulk Ti isotope compositions of ordinary and enstatite chondrites due to potential small-scale heterogeneities. Although the observed $\delta^{49}\text{Ti}$ variations in chondrites may reflect sample heterogeneity, the present dataset does not allow excluding the presence of analytical artefacts.

To better determine the Ti isotope composition of the chondritic reservoir and constrain the sources of inter-laboratory variations, an inter-comparison study is required. For this purpose, ordinary chondrites are particularly suitable, because (i) they are characterised by small, rather uniform nucleosynthetic Ti variations (Trinquier et al., 2009; Williams et al., 2021; Zhang et al., 2012), hence mitigating uncertainties related to the correction for mass-independent isotope compositions. (ii) Ordinary chondrites are the most abundant type of meteorites, which allows for analysis of large sample sizes

representative of the bulk composition in a suite of different meteorites. (iii) They may be more representative of the BSE compared to carbonaceous chondrites since the Earth accreted only limited amounts of carbonaceous chondrite-like material (e.g. Budde et al., 2019; Mezger et al., 2020; Schönbachler et al., 2010). Here, $\delta^{49}\text{Ti}$ data for 10 ordinary chondrites and various geochemical reference materials were determined by an interlaboratory comparison conducted in three laboratories. Revised estimates for the Ti isotope composition of the chondritic reservoir and the BSE are presented.

2. Samples

Ten ordinary chondrites were selected for Ti isotope analysis. The sample set comprises chondrites from the H (Allegan, Estacado, Pultusk, Richardton, St. Marguerite, Zag), L (Farmington, Saratov) and LL (Dhurmsala) groups, as well as the H/L chondrite Tieschitz. The samples were distributed as powders, fused glasses, and aliquots of a Parr bomb dissolved meteorite (Table 1). Powder aliquots originate mostly from 1 to 20 g powdered meteorite fragments (Table S2). Fused glasses are aliquots from the same LiBO_2 pellets previously studied by Greber et al. (2017b).

3. Analytical methods

Titanium isotope data were obtained for ordinary chondrites and terrestrial reference materials at the University of Bern, the Leibniz University Hannover (LUH), and ETH Zurich. The participating laboratories applied a ^{47}Ti - ^{49}Ti double spike technique, each laboratory utilising their own specific spikes, various sample digestion techniques and procedures to isolate Ti from matrix elements. A brief description of the methods is given below and summarised in Table 2.

Titanium isotope data are reported in the delta notation relative to the OL-Ti standard (Millet and Dauphas, 2014):

$$\delta^{49}\text{Ti} (\text{‰}) = \left[\frac{{}^{49}\text{Ti}/{}^{47}\text{Ti}_{\text{Sample}}}{{}^{49}\text{Ti}/{}^{47}\text{Ti}_{\text{OL-Ti}}} - 1 \right] \times 1000$$

3.1. Titanium isotope analysis at the University of Bern

The analytical technique for the Ti isotope measurements of chondrites at the University of Bern used the digestion technique and separation procedure as published in Greber et al. (2017b, 2021) and Zhang et al. (2011), but with a newly produced ^{47}Ti - ^{49}Ti double spike (further information on the double spike are given in the supplementary material). Around 100 mg of all samples provided as powders (i.e. Allegan, Estacado, Richardton, Zag) were fluxed together with 600 mg of ultrapure lithium metaborate (LiBO_2) from SCP Science at ca. 1100 °C for 10 min in graphite crucibles. The resulting glass pellets were fragmented

Table 1
Overview of chondrites analysed for Ti isotopes.

Sample	Chondrite group	Recovery	Distributed material	Laboratory
Allegan	H5	fall	powder	Bern, Hannover, Zurich
Estacado	H6	find	powder	Bern, Hannover, Zurich
Pultusk	H5	fall	fused glass ^a	Zurich
Richardton ^b	H5	fall	powder + Parr bomb-dissolved aliquot ^c	Bern, Hannover, Zurich
St. Marguerite	H4	fall	fused glass ^a	Bern, Hannover, Zurich
Zag	H3-6	fall	powder	Bern, Hannover, Zurich
Farmington	L5	fall	fused glass ^a	Bern
Saratov	L4	fall	powder	Zurich
Dhurmsala	LL6	fall	fused glass ^a	Bern, Hannover
Tieschitz	H/L3.6	fall	powder	Zurich

^a Aliquots of the same LiBO_2 pellets studied by Greber et al. (2017b).

^b Aliquots of the same sample powder studied by Williams et al. (2021).

^c Dissolved at ETH Zurich.

Table 2

Analytical techniques used by the different laboratories.

Laboratory	Digestion method	Separation procedure	Instrument, sample introduction system, acid matrix	Reproducibility (2SD)
Bern	alkali flux fusion	2-step procedure ^a Eichrom TODGA, Bio-Rad AG1-X8	Neptune (HR) Aridus III 0.5 M HNO ₃ -0.005 M HF	±0.035 ‰ ^d
Hannover	high-pressure digestion	5-step procedure ^b Bio-Rad AG50W-X8, AG1-X8; Eichrom Ln	Neptune Plus (HR) Aridus II 0.3 M HNO ₃ -0.0015 M HF	±0.049 ‰ ^e
Zurich	high-pressure digestion	3-step procedure ^c Bio-Rad AG1-X8	Neptune Plus (MR, HR) Aridus II 0.5 M HNO ₃ -0.015 M HF	±0.024 ‰ ^f

2SD reproducibility of $\delta^{49}\text{Ti}$ based on 2SD for GSP-2^d, JB-2^e and BHVO-2^f (Table S3).^a Zhang et al. (2011).^b Rzehak et al. (2021).^c Williams et al. (2021), Anguelova et al. (2022).

and clean aliquots containing between 4 and 8 μg Ti were weighed into Savillex beakers and mixed with ^{47}Ti – ^{49}Ti double spike. The three samples, (i.e. Dhurmsala, Farmington and St. Marguerite) that were already provided as splits from the same LiBO₂ pellets as used in Greber et al. (2017b), and the Parr bomb dissolved Richardton chondrite from ETH Zurich, were also spiked. All samples measured in this study have double spike-sample proportions in the preferred spike range as defined in the supplementary material. The sample-spike mixtures were then dissolved in 10 ml of 3 M HNO₃ at 140 °C, dried down and re-digested in 5 ml 12 M HNO₃ to achieve sample-spike equilibration. Titanium was then isolated from the matrix with a two-step separation procedure. During the first step, Ti was separated from the matrix on a 2 ml Eichrom TODGA column, and during the second step, the Ti fraction was purified using a 0.8 ml AG1-X8 Bio-Rad column.

The Ti isotopes were then measured on a Thermo Fisher Scientific Neptune Plus multi-collector inductively coupled plasma mass spectrometer (MC-ICP-MS) at the University of Bern. The purified samples were dissolved in 0.5 M HNO₃-0.005 M HF and introduced into the instrument using an Aridus III desolvating nebuliser system equipped with a 0.2 mm capillary. Titanium isotopes were measured using Faraday cups equipped with 10¹¹ Ω resistors at masses 46, 47, 48, 49 and 50, together with mass 44 to monitor ^{44}Ca and to allow for interference correction of ^{46}Ca and ^{48}Ca on ^{46}Ti and ^{48}Ti , respectively. As several of the measured isotopes are impacted by polyatomic interferences (e.g., $^{14}\text{N}_2^{16}\text{O}$ on ^{44}Ca , $^{30,29,28}\text{Si}$, $^{16,17,18}\text{O}$ on ^{46}Ti and $^{36}\text{Ar}^{14}\text{N}$ on ^{50}Ti) measurements were performed in high resolution on the plateau with the lowest mass. Measurements consist of 100 cycles with an integration time of 4.194 s. The ion intensity of the pure solvent was measured at the beginning of every sequence and subsequently after every 6 to 12 measurements for on peak zero correction. Each sample was bracketed by a measurement of the OL-Ti standard spiked at the same level as the samples with ^{48}Ti signal intensities matching to $\pm 10\%$ between samples and standards.

Data reduction to obtain $\delta^{49}\text{Ti}$ values was done offline with a Mathematica script that included (i) on peak zero correction, (ii) interference correction of ^{46}Ca and ^{48}Ca on ^{46}Ti and ^{48}Ti , respectively, (iii) double spike deconvolution and (iv) standard sample bracketing (SSB) following the method described in Greber et al. (2017b) and Greber and Van Zuilen (2022). The double spike deconvolution utilised the measured $^{46}\text{Ti}/^{47}\text{Ti}$, $^{48}\text{Ti}/^{47}\text{Ti}$ and $^{49}\text{Ti}/^{47}\text{Ti}$ ratios, avoiding ^{50}Ti as it is impacted by ^{50}Cr and ^{50}V interferences and exhibits the largest mass-independent Ti isotope variations in meteorites (Leya et al., 2008; Trinquier et al., 2009; Zhang et al., 2012; Williams et al., 2021). Each sample was measured between 3 and 5 times and the averages are reported as the final $\delta^{49}\text{Ti}$ values. In addition, the Ti isotope compositions of eight geochemical reference materials are reported (OKUM, DTS-2,

RGM-2, BIR-1a, BHVO-2, BCR-2, AGV-2). These reference materials have different Ti concentrations and major element compositions and were processed identically to the chondrite samples. The resulting $\delta^{49}\text{Ti}$ values of the geostandards agree well with those published, except for standard GSP-2 ($\delta^{49}\text{Ti} = +0.475 \pm 0.035\%$, 2SD). This $\delta^{49}\text{Ti}$ composition is heavier than that previously reported ($+0.383 \pm 0.045$ and $+0.373 \pm 0.072\%$; He et al., 2020, 2022). However, our value for GSP-2 agrees well with that measured by the Hannover laboratory of $+0.494 \pm 0.020\%$ (2SD) (Table S3) in the framework of this study. This may indicate that heterogeneous batches of GSP-2 exist with respect to their Ti isotopic compositions. We argue that the $\delta^{49}\text{Ti}$ value of $+0.475 \pm 0.035\%$ for our GSP-2 reference material is accurate, as this value was verified independently through the measurement of another GSP-2 reference material at the Leibniz University Hannover.

To test whether our method produces accurate results for samples with low Ti concentrations, we measured the reference material DTS-2, a dunite that contains 120 $\mu\text{g/g}$ Ti. As a comparison, chondrites typically have Ti concentrations between 600 $\mu\text{g/g}$ and 680 $\mu\text{g/g}$. DTS-2 yielded an $\delta^{49}\text{Ti}$ of $-0.063 \pm 0.036\%$ (2SD, $n = 2$), within uncertainties identical to the proposed value of $-0.047 \pm 0.025\%$ by Li et al. (2022).

Finally, the analytical uncertainty of Ti isotope data obtained at the University of Bern is $\pm 0.035\%$, estimated based on the 2SD reproducibility of 20 analyses of the reference material GSP-2.

3.2. Titanium isotope analysis at the Leibniz University Hannover (LUH)

Samples were prepared in the clean lab facility of the geochemistry group of LUH. A detailed description of the chemical separation procedure of Ti is reported in Kommescher et al. (2020) and Rzehak et al. (2021). All dilutions were prepared with Merck Milli-Q 18.2 M Ω -cm grade H₂O and purified acids. Nitric acid and HCl were purified from p. a. grade reagents using Savillex DST-1000 sub-boiling and quartz stills. Ultrapure grade HF (Ultrex II, J.T.Baker) was used. Powdered, Parr bomb dissolved (Richardton, ETH Zurich), or fused aliquots (previously studied by Greber et al., 2017b) of meteorite samples were processed in the clean lab facility of the geochemistry group of LUH. Samples were weighed in the beaker resulting in 4–140 μg of Ti per sample. In addition, two geochemical reference materials (JB-2 and BCR-2) and a procedural blank were included.

Aliquots of fused glasses and the Parr bomb digested Richardton chondrite were dissolved in 4 ml of 3 M HNO₃-0.2 M HF. Powdered aliquots were digested following the protocol of Braukmüller et al. (2020). Samples were attacked with a 1:1 mixture of 14 M HNO₃ and 24 M HF (closed, 120 °C for 24 h), dried down at 90 °C and re-dissolved in the same acid mixture in Parr bombs at 180 °C for 3 days. Subsequently, the samples were evaporated to dryness at 90 °C and dissolved in 4 ml of

3 M HNO₃-0.2 M HF. Approximate concentrations for spike addition were determined for Dhurmsala, St. Marguerite, Richardton, Allegan, Zag, and Estacado using a Thermo Scientific Element XR ICP-MS at LUH. Samples were then spiked in the appropriate sample-spike proportion using an aliquot of the Cologne ⁴⁹Ti/⁴⁷Ti double spike (optimal sample-spike Ti ratio = 0.51:0.49; see Kommescher et al., 2020) and allowed to equilibrate for 24 h. After equilibration, samples were dried down to incipient dryness and refluxed with 6 M HCl. Following subsequent dry down, samples were dissolved in 1.5 M HCl-2 % H₂O₂ for chemistry prior to loading onto the columns. Upon visual inspection all samples were completely dissolved. After centrifugation, samples were loaded onto pre-cleaned and conditioned columns in 1.5 M HCl-2 % H₂O₂. Titanium was purified using a five-step column chemistry modified after Tusch et al. (2019), which is described in greater detail in Rzehak et al. (2021). Essentially, the use of 1.5 M HCl-2 % H₂O₂ keeps Ti in solution, while various resins separate matrix elements. After column chemistry, samples were dried down and then refluxed in 6 M HNO₃-0.1 M HF and H₂O₂ in a 9:1 mixture to remove remaining organic residues originating from the resin. Once dried, samples were re-dissolved in 0.3 M HNO₃-0.0015 M HF for Ti isotope analysis.

Samples were measured using an upgraded Thermo Scientific Neptune MC-ICP-MS. Sample solutions were introduced via an Aridus II desolvating system (plus additional Ar and N₂ gas). The instrument was fitted with Ni sample and Ni (H) skimmer cones. Lens and gas settings were adjusted daily and mass resolving power was in the range of ~9,000 ($m/(m_{0.95}-m_{0.05})$) in high-resolution mode. At the beginning, middle, and end of each sequence multiple spiked aliquots of the OL-Ti reference material and the synthetic in-house reference material ColTi were measured to account for long-term drifts and unresolved polyatomic interferences. In addition to synthetic reference materials, each sequence contained at least one spiked and chemically processed geochemical reference material, which was measured before and after each sample to evaluate the intermediate precision. The instrument setup is the same as in Kommescher et al. (2020) and Rzehak et al. (2021). Sample solutions contained at least 1 µg/mL of Ti resulting in ion beam intensities of ca. 0.5, 3.5, 5.5 and 3.9 × 10⁻¹¹ A for 10¹¹ Ω amplifiers and ⁴⁶Ti, ⁴⁷Ti, ⁴⁸Ti and ⁴⁹Ti, respectively. The solution used for analyses (“on peak zero”) gave background intensities that were a factor of 1,000 lower, ca. 0.4, 2, 3 and 2 × 10⁻¹⁴ A for ⁴⁶Ti, ⁴⁷Ti, ⁴⁸Ti and ⁴⁹Ti, respectively. All ion beams were collected using 10¹¹ Ω amplifiers. Each analysis included the measurement of 60 cycles with 8.4 s integration time each. Data reduction was performed offline using an iterative method based on Compston and Oversby (1969), improved by Heuser et al. (2002) and Schönberg et al. (2008). Measurements of spiked aliquots of the OL-Ti and ColTi solutions give average values of +0.001 ± 0.035 ‰ (2SD, n = 9) and +0.229 ± 0.034 ‰ (2SD, n = 15). This corresponds to a 95 % confidence interval (CI, calculated using the t-factor for n-1 degrees of freedom, i.e. analyses, times the standard error) of ±0.014 ‰ and ±0.009 ‰, respectively. A δ⁴⁹Ti value of +0.494 ± 0.020 ‰ (2SD, n = 4; 95 % CI = 0.016 ‰) was obtained for the GSP-2 standard (Table S3). The reproducibility (2SD) is estimated at ± 0.049 ‰ based on repeat analyses (n = 6) of JB-2 (δ⁴⁹Ti = -0.024 ± 0.049 ‰, 95 % CI = 0.026 ‰, Table S3). Total procedural blanks were below 30 ng Ti, contributing less than 1 % to the processed sample Ti, and are thus negligible. Three samples (BCR-2, Dhurmsala, St. Marguerite) were erroneously spiked and yielded inaccurate results (Table S4).

3.3. Titanium isotope analysis at ETH Zurich

Sample processing and analysis at ETH Zurich followed the protocols outlined in Williams et al. (2021) and Anguelova et al. (2022). Approximately 100 mg of powdered meteorite and geochemical reference material were dissolved in a mixture of concentrated HF and HNO₃ in Parr bombs at 170 °C for 4.5 days. Following digestion, sample solutions were evaporated to dryness, taken up in 20 ml 6 M HCl and

refluxed overnight at 120 °C to decompose precipitated fluorides. At this stage, the Richardton chondrite was equally split into multiple aliquots for further processing in each laboratory. Digestion of the Saratov and Tieschitz chondrites, however, followed a different protocol in order to enable further processing for Cr isotope analysis. The two samples were dissolved using concentrated HF and HNO₃ in high-pressure, octagonal body PFA vials in an oven at 155 °C for 3 days. The solutions were subsequently dried down, re-dissolved in concentrated HCl and placed in an oven at 155 °C for another 3 days. Finally, the samples were repeatedly treated with 6 M HCl until clear solutions were obtained. Fused glasses (i.e. St. Marguerite and Pultusk) were dissolved in 5 ml 6 M HCl. Titanium concentrations were determined using a Thermo Scientific Element XR ICP-MS and aliquots containing 3–20 µg Ti were mixed 1:1 with a ⁴⁷Ti-⁴⁹Ti double spike (Williams et al., 2021). Spiked aliquots were refluxed overnight, dried down and re-dissolved in 6 M HCl twice to achieve sample-spike equilibrium. Purification of Ti followed the method of Williams et al. (2021). Titanium was separated from the matrix via a three-step ion-exchange chromatography using Bio-Rad AG1-X8 anion exchange resin (200–400 mesh, chloride form). Aliquots of fused glasses were split over multiple columns in order to reduce B/F ratios in the sample solution. Total procedural blanks were less than 2 ng and are thus considered insignificant.

Titanium isotope analyses were performed on a Thermo Scientific Neptune Plus MC-ICP-MS at ETH Zurich using an Aridus II desolvating nebuliser system. Samples and standards were dissolved in 0.5 M HNO₃-0.015 M HF. Standard sample and X skimmer cones were used. Measurements were carried out in medium- and high-resolution modes on the low-mass peak-shoulder to avoid polyatomic interferences. Each sample analysis was bracketed by measurements of an equivalently spiked Ti Alfa Aesar wire in-house standard (Williams et al., 2021) and concentrations for samples and standard were matched within 10 %. Isotope data were acquired in 40 measuring cycles (8.4 s integration time) in static mode, using 10¹¹ Ω amplifiers for ⁴⁶Ti, ⁴⁷Ti, ⁴⁸Ti, ⁴⁹Ti and ⁵⁰Ti and 10¹² Ω amplifiers for ⁴⁴Ca and ⁹⁰Zr⁺⁺, which is monitored at half mass 45. Backgrounds were recorded on-peak in pure 0.5 M HNO₃-0.015 M HF solution before each analysis. Background and Ca-interference corrections were performed offline. Double spike data reduction was carried out offline and follows the procedure of Siebert et al. (2001), using the intensities of ⁴⁶Ti, ⁴⁷Ti, ⁴⁸Ti and ⁴⁹Ti. Titanium isotope compositions were determined relative to the in-house Ti Alfa Aesar wire standard by SSB and re-scaled to the OL-Ti standard by applying a systematic offset of 0.224 ‰ (Williams et al., 2021).

Methods have been optimised compared to Williams et al. (2021) by (i) recalibrating the double spike set up in 2013, (ii) tight matching of spike/sample ratios for samples and bracketing standards, (iii) improved quality control regarding sample purity (e.g. Ca) and (iv) analysis of known samples before measuring unknown ones. The Ti isotope compositions of geochemical reference materials (BHVO-2, BCR-2, GP13), that were processed together with the chondrite samples, are within uncertainties identical to published values (e.g. Deng et al., 2018b; Greber et al., 2017b; 2021; Millet et al., 2016) and data reported in this study (Table S3). GP13 is a peridotite with a Ti concentration of 720 µg/g, resembling the chemical composition of chondrites (600–680 µg/g Ti). The accuracy of δ⁴⁹Ti results for small quantities of processed Ti was further verified in the recent study of Anguelova et al. (2022) based on 1.5–20 µg Ti sample aliquots of a peridotite reference material (UB-N).

The 2SD reproducibility is estimated at ±0.024 ‰ based on repeat analyses (n = 17) of BHVO-2 and is similar to the long-term analytical precision of our method of ±0.025 ‰ (2SD) based on 65 measurements of BHVO-2 over the course of 3 years.

3.4. Correction for nucleosynthetic Ti isotope variations

The application of the double spike technique relies on the intrinsic assumption that the difference in the isotopic composition between a sample and the standard is purely mass-dependent. This condition is,

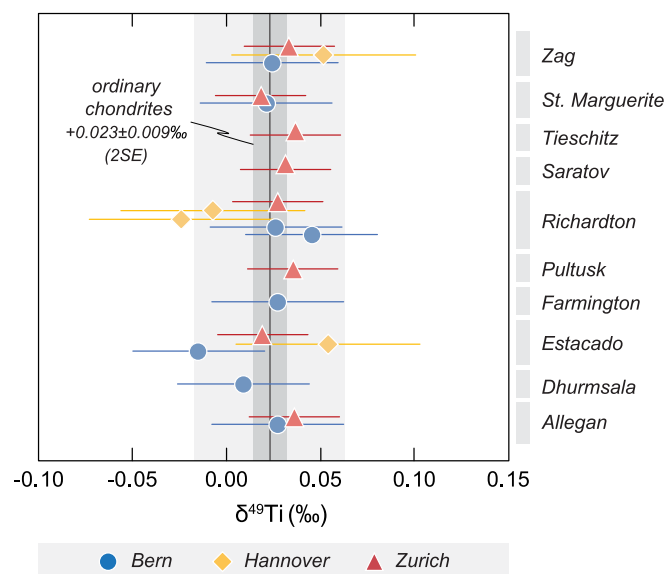


Fig. 1. Ordinary chondrites measured in this study. Uncertainties are the 2SD reproducibility of the respective laboratories (Tables 2 and 3). All chondrites are characterised by a homogeneous and inter-laboratory consistent Ti isotope composition, averaging at $+0.023 \pm 0.009$ ‰ (2SE). Bars around the mean value are the 2SD (bright grey) and the 2SE (dark grey).

however, not met for extra-terrestrial materials, which also display mass-independent isotope variations of nucleosynthetic origin that need to be accounted for. Small nucleosynthetic Ti isotope variations are recorded in ordinary chondrites (e.g. [Trinquier et al., 2009](#); [Williams et al., 2021](#); [Zhang et al., 2012](#)). The mass-dependent Ti isotope compositions of the chondrite samples, therefore, need to be corrected for shifts in $\epsilon^{46}\text{Ti}$ and $\epsilon^{48}\text{Ti}$ (i.e. the parts per 10,000 deviations of the $^{46}\text{Ti}/^{47}\text{Ti}$ and $^{48}\text{Ti}/^{47}\text{Ti}$ ratios from a terrestrial standard corrected for mass-dependent fractionation). Because ordinary chondrites display limited inter- and intra-group variations in nucleosynthetic Ti isotope compositions (e.g. [Rüfenacht et al., 2023](#); [Trinquier et al., 2009](#); [Williams et al., 2021](#); [Zhang et al., 2012](#); Table S5), correction was performed using average $\epsilon^{46}\text{Ti}$ and $\epsilon^{48}\text{Ti}$ values from the literature (-0.14 ± 0.04 and -0.01 ± 0.08 , $n = 20$, 1SD; Table S5) following the protocol of [Williams et al. \(2021\)](#). The applied correction translates into a $\delta^{49}\text{Ti}$ shift of -0.014 ‰ and introduces a negligible increase of the uncertainty on $\delta^{49}\text{Ti}$.

4. Results

Titanium isotope compositions of chondrites and geochemical reference materials are presented in Fig. 1, Tables 3, 4 and S3. Chondrite Ti isotope data from all laboratories agree well within the quoted analytical uncertainty (Fig. 1, Table 3). The average Ti isotope composition defined by all ordinary chondrites of this study is $\delta^{49}\text{Ti} = +0.023 \pm 0.009$ ‰ (2SE, $n = 20$).

The analytical uncertainty of the Ti isotope data, expressed as 2SD of the most frequently measured geochemical reference material of each laboratory (Tables 2, S3), is mirrored by the $\delta^{49}\text{Ti}$ spread of the chondrites analysed, i.e. it is largest for the Leibniz University Hannover and smallest for ETH Zurich (Fig. S2). The $\delta^{49}\text{Ti}$ averages of ordinary chondrites determined at the University of Bern ($+0.019 \pm 0.012$ ‰, 2SE, $n = 8$), the Leibniz University Hannover ($+0.018 \pm 0.040$ ‰, 2SE, $n = 4$), and ETH Zurich ($+0.028 \pm 0.005$ ‰, 2SE, $n = 8$) (Table 4) overlap within their 2SE and, consequently, these datasets do not show a statistically significant difference in their mean or median values when applying a Student's *t*-test or Mann-Whitney *U* Test (two-tailed, significance level 0.05). Furthermore, the mean square weighted deviation (MSWD) of all chondrites (analytical uncertainties from geochemical

reference materials) yields 1.08. The fact that three laboratories with different methodologies obtain identical $\delta^{49}\text{Ti}$ averages for bulk chondrites indicates accurate analytics. A MSWD of 1.08 further suggests accurate estimates of uncertainties.

Different sample digestion methods were used by the participating laboratories. Two laboratories (Leibniz University Hannover, ETH Zurich) utilised high-pressure acid digestion, whereas one laboratory (University of Bern) applied a flux fusion technique. Both high-pressure acid digestion and flux fusion ensure complete decomposition of refractory phases such as chromite, which is a common accessory in ordinary chondrites and typically contains 2–3 wt% TiO_2 (e.g., [Wlotzka, 2005](#)). Notably, each laboratory reports identical $\delta^{49}\text{Ti}$ values within uncertainties for aliquots of the Richardton chondrite that were distributed as both rock powder and Parr bomb pre-digested material (Table 3). It can, therefore, be concluded that the sample digestion protocols utilised in this study do not cause any measurable Ti isotope bias.

Titanium isotope data for the chondrites Dhurmsala, Farmington, Pultusk, Richardton, and St. Marguerite are within the uncertainties of previously reported $\delta^{49}\text{Ti}$ values ([Greber et al., 2017b](#); [Williams et al., 2021](#); Fig. S3).

5. Discussion

5.1. Comparison with literature data

Previously published Ti isotope data for bulk chondrites showed significant inter-laboratory variations, with $\delta^{49}\text{Ti}$ averages ranging from $+0.007 \pm 0.010$ ‰ (2SE, [Greber et al., 2017b](#)) to $+0.071 \pm 0.018$ ‰ (2SE, [Deng et al., 2018b](#)) (Fig. 2, S4). While the $\delta^{49}\text{Ti}$ estimates provided by [Greber et al. \(2017b\); \$+0.007 \pm 0.010\$ ‰ and \[Williams et al. \\(2021\\); \\$\delta^{49}\text{Ti} = +0.047 \pm 0.029\\$ ‰ agree within 2SE with the value proposed here \\(\\$+0.023 \pm 0.009\\$ ‰; Fig. 2, Table 4\\), \\$\delta^{49}\text{Ti}\\$ averages from \\[Deng et al. \\\(2018b\\\); \\\$+0.071 \pm 0.018\\\$ ‰ and \\\[Deng et al. \\\\(2023\\\\); \\\\$+0.053 \pm 0.005\\\\$ ‰ are different \\\\(Student's *t*-test \\\\$p\\\\$ -value \\\\$< 0.0001\\\\$ \\\\).\\\]\\\(#\\\)\\]\\(#\\)\]\(#\)](#)

Notably, such an inter-laboratory $\delta^{49}\text{Ti}$ discrepancy is not evident for geochemical reference materials. For example, the Ti isotope data for all four reference materials reported by [Deng et al. \(2023\) \(i.e. BHVO-2, BCR-2, BIR-1, AGV-2\) agree to within \$\pm 0.010\$ ‰ with our data. However, these samples are of basaltic-andesitic composition with higher Ti concentrations \(\$>6300\$ \$\mu\text{g/g}\$ \) than chondrites \(typically 600–680 \$\mu\text{g/g}\$ \). It is therefore possible that the larger scatter in the available chondrite data reflects the increased analytical challenge to accurately measure samples with low Ti contents. To address this issue, we analysed the geochemical reference materials OKUM \(University of Bern, komatiite with 2300 \$\mu\text{g/g}\$ Ti\), DTS-2 \(University of Bern, dunite with 120 \$\mu\text{g/g}\$ Ti\) and GP13 \(ETH Zurich, peridotite with 720 \$\mu\text{g/g}\$ Ti\) that are closer to chondrites in their Ti concentrations \(Table S3\). While we are not aware of published data for OKUM, results for GP13 \(\$+0.033 \pm 0.033\$ ‰\) and DTS-2 \(\$-0.063 \pm 0.036\$ ‰\) agree with previous data \(\$+0.007 \pm 0.022\$ ‰, \[Millet et al., 2016\]\(#\); \$-0.047 \pm 0.025\$ ‰, \[Li et al., 2022\]\(#\)\). This further corroborates that the analytical methods applied here produce accurate results. It is also noteworthy that minor impurities in the double spike solution used can cause a small, but resolvable \$\delta^{49}\text{Ti}\$ bias, as described in \[Deng et al. \\(2018b\\) and \\[Deng et al. \\\(2019\\\), requiring a correction of their data. However, the effect of such an impurity on the \\\$\delta^{49}\text{Ti}\\\$ data can depend on the Ti concentration of the sample, and could therefore be more severe for low-Ti samples like chondrites.\\]\\(#\\)\]\(#\)](#)

In summary, it is still unclear why the chondrite Ti isotope data reported by [Deng et al. \(2018b\) and \[Deng et al. \\(2023\\) do not agree with the \\$\delta^{49}\text{Ti}\\$ estimate of \\$+0.023 \pm 0.009\\$ ‰ \\(2SE\\) proposed here, requiring further improvement of the analytical techniques and inter-laboratory calibrations.\]\(#\)](#)

Table 3
Titanium isotope compositions of chondrites measured in this study.

Sample/lab	Group	$\delta^{49}\text{Ti}_{\text{meas}}$ (‰) ^a	$\delta^{49}\text{Ti}$ (‰)	2SD ^b	Reproducibility (2SD) ^c	N ^d
<i>Allegan</i>	H5					
Bern		0.040	0.025	0.040	0.035	5
Zurich		0.049	0.035	0.031	0.024	7
average		0.044	0.030	0.013		n = 2
<i>Dhurmsala</i> ^e	LL6					
Bern		0.022	0.007	0.034	0.035	3
<i>Estacado</i>	H6					
Bern		−0.002	−0.015	0.030	0.035	3
Hannover		0.067	0.053	0.048	0.049	4
Zurich		0.032	0.018	0.016	0.024	8
average		0.033	0.018	0.069		n = 3
<i>Farmington</i> ^e	L5					
Bern		0.040	0.026	0.023	0.035	3
<i>Pultusk</i> ^e	H5					
Zurich		0.048	0.034	0.013	0.024	3
<i>Richardton</i> ^f	H5					
Bern-a		0.058	0.043	0.028	0.035	5
Bern-b ^g		0.039	0.025	0.026	0.035	5
Hannover-a		0.006	−0.008	0.017	0.049	4
Hannover-b ^g		−0.011	−0.025	0.005	0.049	4
Zurich		0.040	0.026	0.024	0.024	8
average		0.026	0.012	0.056		n = 5
<i>Saratov</i>	L4					
Zurich		0.044	0.030	0.013	0.024	3
<i>St. Marguerite</i> ^e	H4					
Bern		0.034	0.019	0.025	0.035	5
Zurich		0.031	0.017	0.025	0.024	2
average		0.033	0.018	0.003		n = 2
<i>Tieschitz</i>	H/L3.6					
Zurich		0.050	0.035	0.026	0.024	3
<i>Zag</i>	H3–6					
Bern		0.037	0.023	0.048	0.035	4
Hannover		0.065	0.051	0.038	0.049	4
Zurich		0.046	0.032	0.026	0.024	8
average		0.049	0.035	0.029		n = 3

MSWD of all measurements = 1.08 using 2SD reproducibility^c.

^a $\delta^{49}\text{Ti}$ prior to correction for nucleosynthetic anomalies.

^b 2SD of N repeat measurements of sample solution.

^c Reproducibility of the respective laboratory estimated from measured geochemical reference materials (see text and Tables 2 and S3).

^d N: number of repeat measurements of sample solution, n: number of samples analysed.

^e Aliquots of the same LiBO₂ pellets studied by Greber et al. (2017b).

^f Aliquots of the same sample powder studied by Williams et al. (2021).

^g Dissolved at ETH Zurich.

Table 4
Average Ti isotope composition of ordinary chondrites.

Laboratory	$\delta^{49}\text{Ti}$ (‰)	2SD	2SE	n
<i>Chondritic average defined by each lab</i>				
Bern	0.019	0.035	0.012	8
Hannover	0.018	0.080	0.040	4
Zurich	0.028	0.015	0.005	8
Chondritic average ⁺	0.023	0.040	0.009	20

n: number of samples analysed.

⁺ Average Ti isotope composition of all chondrites measured in this study.

5.2. The Titanium isotope composition of the chondritic reservoir

5.2.1. Non-carbonaceous chondrites

Ordinary chondrites of different subgroups (H, L, LL) and petrologic types, i.e. different metamorphic grades, (3–6) are characterised by

relatively homogeneous Ti isotope compositions (Table 3). Considering the average $\delta^{49}\text{Ti}$ values determined for each sample, all chondrites analysed in this study display identical $\delta^{49}\text{Ti}$ values within uncertainties. These results suggest (i) negligible Ti isotope fractionation associated with thermal metamorphism at the sampling scale and (ii) further support a homogeneous inner Solar System with respect to mass-dependent Ti isotopes. The Ti isotope data of enstatite chondrites (Deng et al., 2018b, 2023; Greber et al., 2017b; Table S6) also overlaps with the chondritic $\delta^{49}\text{Ti}$ average reported here. Hence, our newly defined average Ti isotope composition of ordinary chondrites ($+0.023 \pm 0.009$ ‰, 2SE, n = 20) provides a robust baseline for tracing the differentiation history of planetary reservoirs in the inner Solar System.

5.2.2. Carbonaceous chondrites

Previous studies reported Ti isotope data for chondrites of different classes. Despite the presence of inter-laboratory variations, carbonaceous chondrites appear to display subtle, yet statistically not resolvable

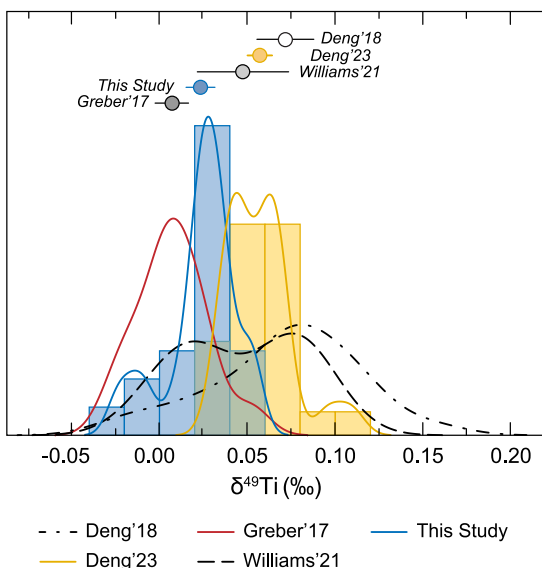


Fig. 2. Kernel distribution diagrams of published $\delta^{49}\text{Ti}$ data of chondrites (Deng et al., 2018b; 2023; Greber et al., 2017b; Williams et al., 2021) compared with data from this study. For data from this study and from Deng et al. (2023), also the histograms are shown. Data points above the Kernel distributions are the average chondritic Ti isotope compositions ($\pm 2\text{SE}$) of various publications.

enrichments in heavy Ti isotopes relative to enstatite and most ordinary chondrites (Fig. S4 Table S6; Deng et al., 2018b, 2023; Greber et al., 2017b; Williams et al., 2021). Carbonaceous chondrites, in particular CM, CO, and CV type chondrites, contain refractory inclusions (i.e. CAIs) (Hezel et al., 2008) that (i) may host a considerable proportion of the bulk Ti budget and (ii) display distinct nucleosynthetic Ti isotope compositions compared to other meteorite groups (Davis et al., 2018; Leya et al., 2009; Rufenacht et al., 2023; Shollenberger et al., 2022; Torrano et al., 2019; Trinquier et al., 2009; Williams et al., 2021). This increases the risk of erroneous corrections of $\delta^{49}\text{Ti}$ for nucleosynthetic $\epsilon^{46}\text{Ti}$ and $\epsilon^{48}\text{Ti}$ variations. A thorough assessment of these error sources, hence, requires obtaining both nucleosynthetic and mass-dependent Ti isotope data from the same sample aliquot. Calcium-aluminium-rich inclusions further exhibit Ti isotope fractionation related to

evaporation and condensation processes (Davis et al., 2018; Niederer et al., 1985; Simon et al., 2017). Davis et al. (2018) presented a comprehensive set of mass-dependent Ti isotope data for CAIs from Allende. While some inclusions extend to both significantly lower and higher $\delta^{49}\text{Ti}$ values than the bulk meteorite, most CAIs display limited Ti isotope fractionation with a median $\delta^{49}\text{Ti}$ of $+0.110\text{‰}$ (Fig. S5a; Davis et al., 2018). Mixing of up to 10 % CAI-like material ($\delta^{49}\text{Ti} = +0.110\text{‰}$, $\text{TiO}_2 = 1.28\text{ wt\%}$; Davis et al., 2018) with a chondrite matrix ($\delta^{49}\text{Ti} = +0.023\text{‰}$, $\text{TiO}_2 = 0.1\text{ wt\%}$) may account for Ti isotope compositions as heavy as ca. $+0.07\text{‰}$ (Fig. S5b). This consideration is, however, subject to considerable uncertainty due to the $\delta^{49}\text{Ti}$ spread in CAIs and bulk carbonaceous chondrites. A comprehensive Ti isotope study targeting both the nucleosynthetic and mass-dependent Ti isotope compositions of carbonaceous chondrites and their components is required in order to identify potential $\delta^{49}\text{Ti}$ differences between carbonaceous and non-carbonaceous chondrites.

5.3. Implications for the Titanium isotope composition of the Bulk Silicate Earth and the evolution of Earth's mantle reservoirs

Previous estimates for the chondritic reservoir ranged from $+0.007 \pm 0.010\text{‰}$ to $+0.071 \pm 0.018\text{‰}$ for $\delta^{49}\text{Ti}$ (2SE; Deng et al., 2018b, 2023; Greber et al., 2017b; Williams et al., 2021), leaving room for debate as to whether the bulk silicate Earth (BSE, $\delta^{49}\text{Ti} = +0.005 \pm 0.005\text{‰}$, Millet et al., 2016) has a chondritic Ti isotope composition. Having defined a precise and inter-laboratory consistent chondritic average (i.e. $+0.023 \pm 0.009\text{‰}$, 2SE), we re-evaluate the Ti isotope composition of the BSE in the light of the growing body of Ti isotope data for mantle-derived samples. Furthermore, a recent study suggested that the Earth's mantle underwent a secular evolution towards lower $\delta^{49}\text{Ti}$ between ca. 3.5 and 2.7 Ga (Deng et al., 2023). Since the $\delta^{49}\text{Ti}$ estimate for chondrites reported by Deng et al. (2023) is higher than the value proposed here, our new results also impact the discussion whether the Earth's mantle has undergone a secular evolution in its Ti isotope composition.

While igneous differentiation produces significant $\delta^{49}\text{Ti}$ variations (e.g. Deng et al., 2019; Hoare et al., 2020; Millet et al., 2016), Ti isotope fractionation during partial melting of the mantle is limited (e.g. Anguelova et al., 2022; Deng et al., 2018a, 2023; Hoare et al., 2022). As such, primitive mantle-derived magmas such as basalts and komatiites are suitable for constraining the Ti isotope composition of the mantle

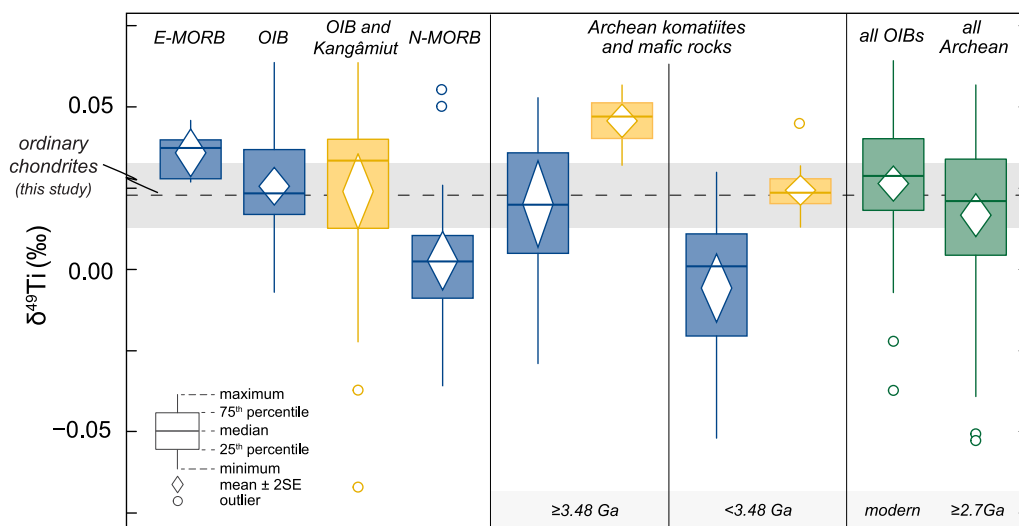


Fig. 3. Comparison of $\delta^{49}\text{Ti}$ literature data for different mantle-derived mafic and komatiitic rocks with the average composition of ordinary chondrites ($+0.023 \pm 0.009\text{‰}$, 2SE) from this study. Data for mantle-derived rocks are from Deng et al. (2018a, 2023), Greber et al. (2017b), Hoare et al. (2020), Johnson et al. (2019), Millet et al. (2016), and Zhao et al. (2020). Yellow whisker plots illustrate the recent data of Deng et al. (2023), blue plots data from all other literature sources and green plots consider all available data. For literature compilation, see supplementary Table S7.

and, hence, that of the BSE. We omit however Ti isotope data for peridotites, because they have been shown to record considerable small-scale mantle heterogeneity associated with metasomatic processes (Anguelova et al., 2022). We further consider arc basalts not representative of the BSE, because their Ti isotope compositions may be affected by sediment recycling (Anguelova et al., 2022), or early crystallisation of Fe-Ti oxides promoted by high oxygen fugacities (Hoare et al., 2020).

Overall, our new $\delta^{49}\text{Ti}$ average for ordinary chondrites agrees well with that of basalts and komatiites (Fig. 3; for literature compilation see supplementary Table S7). Within 2SE, there is no difference in the Ti isotope compositions of E-MORBs ($\delta^{49}\text{Ti} = +0.036 \pm 0.006 \text{ ‰}$; Deng et al., 2018a, Zhao et al., 2020), OIBs ($\delta^{49}\text{Ti} = +0.029 \pm 0.005 \text{ ‰}$; Deng et al., 2023; Hoare et al., 2020; Johnson et al., 2019; Millet et al., 2016; Zhao et al., 2020) and ordinary chondrites ($\delta^{49}\text{Ti} = +0.023 \pm 0.009 \text{ ‰}$, Fig. 1, Table 4). In contrast, N-MORBs ($\delta^{49}\text{Ti} = +0.003 \pm 0.009 \text{ ‰}$; Deng et al., 2018a; Hoare et al., 2020; Millet et al., 2016; Zhao et al., 2020) display slightly lower $\delta^{49}\text{Ti}$ values than ordinary chondrites (Fig. 3).

For komatiites and mafic rocks, however, the situation is more complex, where a shift towards lighter Ti isotope compositions has been observed in pre-3.45 Ga to late-Archean rocks (Greber et al., 2017b; Deng et al., 2018a, 2023). While all studies report a $\delta^{49}\text{Ti}$ shift of a similar magnitude, i.e. 0.022–0.025 ‰, the absolute $\delta^{49}\text{Ti}$ values do not agree (Fig. 3). For example, Greber et al. (2017b) observed a $\delta^{49}\text{Ti}$ shift from $+0.015 \pm 0.013 \text{ ‰}$ to $-0.010 \pm 0.013 \text{ ‰}$ (2SE), whereas Deng et al. (2023) report a transition from $+0.046 \pm 0.005 \text{ ‰}$ to $+0.024 \pm 0.004 \text{ ‰}$ (2SE) (Fig. 3). Notably, the $\delta^{49}\text{Ti}$ difference of ca. 0.03 ‰ between these studies is consistent with the difference between the chondritic average presented here ($\delta^{49}\text{Ti} = +0.023 \pm 0.009 \text{ ‰}$, 2SE) and in Deng et al. (2023; $+0.053 \pm 0.005 \text{ ‰}$, 2SE) (Fig. 2). Two distinct processes have been proposed to explain the $\delta^{49}\text{Ti}$ systematics of komatiites and basalts (N-MORB versus OIB/E-MORB). (i) Greber et al. (2017b) suggested that Ti isotope fractionation during partial melting of the mantle could produce a residue enriched in light Ti isotopes. Magmas from depleted mantle sources such as late-Archean komatiites (e.g. Sossi et al., 2016) and N-MORBs would therefore display lower $\delta^{49}\text{Ti}$ values. However, subsequent experimental data (Rzechak et al., 2021), *ab-initio* calculations (Aarons et al., 2021; Wang et al., 2020) and mantle melting models (Anguelova et al., 2022; Hoare et al., 2022) imply that this effect, if existent, is small ($\Delta^{49}\text{Ti}_{\text{melt-mantle}}$ of around $+0.020 \text{ ‰}$ to $+0.030 \text{ ‰}$). (ii) Alternatively, the slightly lower $\delta^{49}\text{Ti}$ values of Late Archean komatiites and the depleted MORB mantle are interpreted to reflect a secular change in the Ti isotope composition of the mantle due to the progressive recycling of isotopically light residues generated by continental crust extraction during the Middle to Late Archean (Deng et al., 2018a, 2023). Yet, most of the Ti isotope data from Archean mafic and ultramafic rocks span the same $\delta^{49}\text{Ti}$ range as defined by OIBs and N-MORBs. Exceptions are Ti isotope data of pre-3.45 Ga komatiites (Komati) and amphibolites (Isua) reported by Deng et al. (2023), with $\delta^{49}\text{Ti}$ values higher than the chondritic average presented here. Although komatiites are usually well suited to trace the isotope composition of their mantle source (e.g., Dauphas et al., 2010; Greber et al., 2015), further information (i.e. major-, trace element and radiogenic isotope data) is required for a sound data interpretation. Similarly, interpretation of the Ti isotope compositions of the Isua amphibolites is not straightforward, because they may be affected by processes such as crustal recycling, as indicated by trace element systematics (Saji et al., 2018), or Ti isotope fractionation during magmatic differentiation, as reported for metagabbros and amphibolites from the Acasta Gneiss Complex (Aarons et al., 2020).

Although the exact origin of the observed minor mantle heterogeneities remains uncertain, it seems likely that depleted sources such as those sampled by N-MORBs do not reflect the Ti isotope composition of the pristine mantle. In contrast, the within 2SE identical $\delta^{49}\text{Ti}$ of E-MORBs, OIBs and the average of all available Archean mafic and ultramafic samples supports that the BSE has an identical composition to that of ordinary chondrites, which is at the moment best approximated

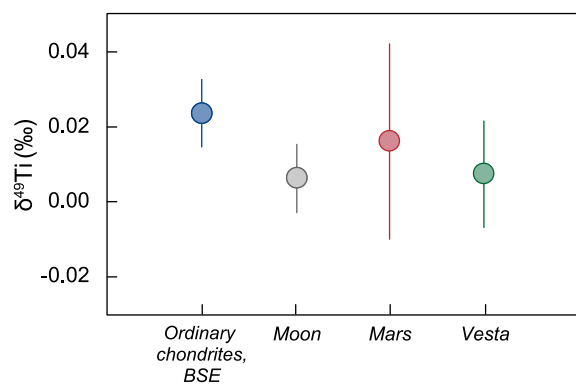


Fig. 4. Titanium isotope estimates for the chondritic reservoir, and thus the bulk silicate Earth (BSE), and other planetary bodies overlap within uncertainties, suggesting the inner Solar System is characterised by a uniform Ti isotope composition. Chondritic reservoir is inferred from ordinary chondrites measured in this study. Estimates for the Moon, Mars and Vesta derived from literature data (Deng et al., 2020; Greber et al., 2017b; Kommescher et al., 2020; Mandl 2019; Millet et al., 2016; Williams et al., 2021; Table S8). Uncertainties are 2SE.

by a $\delta^{49}\text{Ti}$ value of $+0.023 \pm 0.009 \text{ ‰}$. This new BSE estimate combined with literature data of mantle-derived magmas still allows for the interpretation that a shift in the $\delta^{49}\text{Ti}$ value of certain mantle domains occurred between 3.5 Ga and 2.7 Ga as proposed by Deng et al. (2023). However more data, ideally verified by multiple laboratories, is needed to unambiguously verify this finding.

5.4. Titanium isotope homogeneity within the inner Solar System

Differences in the mass-dependent isotope composition between the BSE and chondrites may arise from isotopic fractionation associated with planetary accretion (i.e. impact volatilisation) and differentiation (i.e. core formation) and are reported for several elements, including Mg (e.g. Hin et al., 2017), Si (e.g. Armytage et al., 2011; Moynier et al., 2020), Ni (Klaver et al., 2020), or V (Nielsen et al., 2020). Titanium is a refractory element with a 50 % condensation temperature of 1565 K (Wood et al., 2019). Due to its strongly lithophile character over a wide $f\text{O}_2$ range, Ti is not expected to partition into the cores of planetary bodies, unless differentiation occurs under highly reducing conditions (e.g. Steenstra et al., 2020; Wood and Kiseeva, 2015). The Ti isotope composition of the silicate portions of planetary bodies should therefore be little affected by planetesimal evaporation or core formation, and reflect the composition of the material that condensed from the solar nebula. We propose that the $\delta^{49}\text{Ti}$ of the BSE is indistinguishable from the average Ti isotope composition of ordinary chondrites measured in this study, and further overlaps with those for the Moon, Mars and Vesta derived from low-Ti Mare basalts (Kommescher et al., 2020; Mandl, 2019; Millet et al., 2016), Martian shergottites (Deng et al., 2020; Greber et al., 2017b) and HED meteorites (Greber et al., 2017b; Williams et al., 2021), respectively (Fig. 4). This argues for a uniform inner Solar System with respect to mass-dependent Ti isotopes and is in contrast to the isotopic heterogeneity recently reported for the similarly refractory and lithophile Ca (Zhu et al., 2023).

6. Summary and conclusions

We conducted an inter-comparison Ti isotope study of three laboratories to precisely and accurately determine the mass-dependent Ti isotope composition of the chondritic reservoir. While previous estimates may suffer from heterogeneities at the level of sampling, we have chosen ordinary chondrites (i) to reduce uncertainties associated with the necessary corrections for nucleosynthetic isotope variations, and (ii) to further allow the analysis of large sample sizes representative of the

bulk. The Ti isotope data reported by the different laboratories agree well with each other. All ordinary chondrites, regardless of subgroup (H, L, LL) and petrologic type (3–6), show uniform $\delta^{49}\text{Ti}$ values with a mean $\delta^{49}\text{Ti}$ of $+0.023 \pm 0.009$ ‰ (2SE, $n = 20$).

We further re-evaluated the Ti isotope composition of the bulk silicate Earth in the context of recently published Ti isotope data for mantle-derived samples and show that modern OIBs, E-MORBs and Archean mafic and ultramafic rocks have within uncertainties identical average Ti isotope compositions as ordinary chondrites. This value further overlaps with the estimated Ti isotope compositions of the Moon, Mars and Vesta, suggesting that the inner Solar System is homogeneous with respect to $\delta^{49}\text{Ti}$.

Data availability

Data are available via the Research Collection of ETH Zurich at: <https://doi.org/10.3929/ethz-b000619234>.

CRediT authorship contribution statement

Merislava Anguelova: Conceptualization, Investigation, Writing – original draft, Writing – review & editing. **Nicolas Vilela:** Investigation, Writing – review & editing. **Sebastian Kommescher:** Investigation, Writing – original draft, Writing – review & editing. **Nicolas Greber:** Conceptualization, Investigation, Writing – original draft, Writing – review & editing. **Manuela Fehr:** Conceptualization, Writing – review & editing. **Maria Schönbächler:** Conceptualization, Writing – review & editing.

Declaration of competing interest

The authors declare that they have no known competing financial interests or personal relationships that could have appeared to influence the work reported in this paper.

Acknowledgements

We acknowledge funding of the Swiss National Science Foundation (SNSF) through Project 2 00020.179129 to MA and MS, and Project PCEF2_181172 to NDG. The Neptune MC-ICP-MS at the University of Bern was acquired with funds from the National Centre for Competence in Research PlanetS, also supported by the SNSF. Kevin Burton (Durham University) and Marc-Alban Millet (Cardiff University) are thanked for providing sample material. We are grateful to Marc-Alban Millet for discussions and feedback on the manuscript. We thank Helen Williams for the editorial handling and two anonymous reviewers for their constructive comments.

Appendix A. Supplementary material

The supplementary document contains additional details to the analytical methods for Ti isotope analyses at the University of Bern regarding the Ti double spike calibration and test for optimal sample-spike mixture. This includes Table S1, displaying the composition of the ^{47}Ti - ^{49}Ti double spike at the University of Bern and Figure S1 which shows the Ti isotope composition of the USGS reference material GSP-2 as treated with different amounts of ^{47}Ti - ^{49}Ti double spike at the University of Bern. Table S2 displays the total mass of powdered meteorite for samples that were distributed as powders for the presented calibration study. Figures S2 and S3 provide comparisons of $\delta^{49}\text{Ti}$ chondrite results from the different laboratories involved in this study with a Kernel distribution diagram and with literature results, respectively. Additional data that support the accuracy of the presented $\delta^{49}\text{Ti}$ results is documented in Tables S3 (geochemical reference materials) and Figure S3 (comparison of chondrite aliquots from this study with literature results). Figure S4 provides $\delta^{49}\text{Ti}$ data for chondrites from the

literature. For the discussion of carbonaceous chondrite Ti isotope literature results, Figure S5 displays additional information to the mass-dependent Ti isotope composition of CAIs and mixing of a chondrite-matrix with CAI material in a TiO_2 versus $\delta^{49}\text{Ti}$ mixing diagram. Table S4 shows $\delta^{49}\text{Ti}$ results for three samples that were erroneously spiked and display inaccurate results. Table S5 summarises Ti isotope literature results that are utilised for the correction of $\delta^{49}\text{Ti}$ results for nucleosynthetic Ti isotope variations. Tables S6 and S7 list literature $\delta^{49}\text{Ti}$ results for chondrites (Table S6) and terrestrial samples (Table S7) displayed in Figures 2 and 3. Table S8 presents literature $\delta^{49}\text{Ti}$ data for lunar samples and various meteorites used to estimate the Ti isotope composition of the Moon, Mars and Vesta displayed in Figure 4.

Supplementary material to this article can be found online at <https://doi.org/10.1016/j.gca.2024.01.026>.

References

- Aarons, S.M., Reimink, J.R., Greber, N.D., Heard, A.W., Zhang, Z., Dauphas, N., 2020. Titanium isotopes constrain a magmatic transition at the Hadean-Archean boundary in the Acasta Gneiss Complex. *Sci. Adv.* 6, eabc9959.
- Aarons, S.M., Dauphas, N., Blanchard, M., Zeng, H., Nie, N.X., Johnson, A.C., Greber, N.D., Hopp, T., 2021. Clues from ab initio calculations on titanium isotopic fractionation in tholeiitic and calc-alkaline magma series. *ACS Earth Space Chem.* 5, 2466–2480.
- Anguelova, M., Fehr, M.A., Takazawa, E., Schönbächler, M., 2022. Titanium isotope heterogeneity in the Earth's mantle: a case study of the Horoman peridotite massif. *Geochim. Cosmochim. Acta* 335, 356–368.
- Armtyage, R., Georg, R., Savage, P., Williams, H., Halliday, A., 2011. Silicon isotopes in meteorites and planetary core formation. *Geochim. Cosmochim. Acta* 75, 3662–3676.
- Braukmüller, N., Wombacher, F., Bragagni, A., Münker, C., 2020. Determination of Cu, Zn, Ga, Ag, Cd, In, Sn and Tl in geological reference materials and chondrites by isotope dilution ICP-MS. *Geostand. Geoanal. Res.* 44, 733–752.
- Budde, G., Burkhardt, C., Kleine, T., 2019. Molybdenum isotopic evidence for the late accretion of outer Solar System material to Earth. *Nat. Astron.* 3, 736–741.
- Compston, W., Oversby, V., 1969. Lead isotopic analysis using a double spike. *J. Geophys. Res.* 74, 4338–4348.
- Dauphas, N., Teng, F.Z., Arndt, N.T., 2010. Magnesium and iron isotopes in 2.7 Ga Alexo komatiites: mantle signatures, no evidence for soret diffusion, and identification of diffusive transport in zoned olivine. *Geochim. Cosmochim. Acta* 74, 3274–3291.
- Davis, A.M., Zhang, J., Greber, N.D., Hu, J., Tissot, F.L., Dauphas, N., 2018. Titanium isotopes and rare earth patterns in CAIs: Evidence for thermal processing and gas-dust decoupling in the protoplanetary disk. *Geochim. Cosmochim. Acta* 221, 275–295.
- Deng, Z., Moynier, F., Sossi, P., Chaussidon, M., 2018a. Bridging the depleted MORB mantle and the continental crust using titanium isotopes. *Geochem. Perspect. Lett.* 9, 11–15.
- Deng, Z., Moynier, F., van Zuilen, K., Sossi, P.A., Pringle, E.A., Chaussidon, M., 2018b. Lack of resolvable titanium stable isotopic variations in bulk chondrites. *Geochim. Cosmochim. Acta* 239, 409–419.
- Deng, Z., Chaussidon, M., Savage, P., Robert, F., Pik, R., Moynier, F., 2019. Titanium isotopes as a tracer for the plume or island arc affinity of felsic rocks. *Proc. Natl. Acad. Sci.* 116, 1132–1135.
- Deng, Z., Moynier, F., Villeneuve, J., Jensen, N.K., Liu, D., Cartigny, P., Mikouchi, T., Siebert, J., Agraniar, A., Chaussidon, M., 2020. Early oxidation of the martian crust triggered by impacts. *Sci. Adv.* 6, eabc4941.
- Deng, Z., Schiller, M., Jackson, M.G., Millet, M.-A., Pan, L., Nikolajsen, K., Saji, N.S., Huang, D., Bizzarro, M., 2023. Earth's evolving geodynamic regime recorded by titanium isotopes. *Nature* 621, 100–104.
- Greber, N.D., Puchtel, I.S., Nägler, T.F., Mezger, K., 2015. Komatiites constrain molybdenum isotope composition of the Earth's mantle. *Earth Planet. Sci. Lett.* 421, 129–138.
- Greber, N.D., Dauphas, N., Bekker, A., Ptáček, M.P., Bindeman, I.N., Hofmann, A., 2017a. Titanium isotopic evidence for felsic crust and plate tectonics 3.5 billion years ago. *Science* 357, 1271–1274.
- Greber, N.D., Dauphas, N., Puchtel, I.S., Hofmann, B.A., Arndt, N.T., 2017b. Titanium stable isotopic variations in chondrites, achondrites and lunar rocks. *Geochim. Cosmochim. Acta* 213, 534–552.
- Greber, N.D., Pettke, T., Vilela, N., Lanari, P., Dauphas, N., 2021. Titanium isotopic compositions of bulk rocks and mineral separates from the Kos magmatic suite: Insights into fractional crystallization and magma mixing processes. *Chem. Geol.*
- Greber, N., Van Zuilen, K., 2022. Multi-collector inductively coupled plasma mass spectrometry: new developments and basic concepts for high-precision measurements of mass-dependent isotope signatures. *Chimia* 76, 18–25.
- He, X., Ma, J., Wei, G., Zhang, L., Wang, Z., Wang, Q., 2020. A new procedure for titanium separation in geological samples for $^{49}\text{Ti}/^{47}\text{Ti}$ ratio measurement by MC-ICP-MS. *J. Anal. at. Spectrom.* 35, 100–106.
- He, X., Ma, J., Wei, G., Wang, Z., Zhang, L., Zeng, T., Zhang, Z., 2022. Mass-dependent fractionation of titanium stable isotopes during intensive weathering of basalts. *Earth Planet. Sci. Lett.* 579, 117347.

- Heuser, A., Eisenhauer, A., Gussone, N., Bock, B., Hansen, B., Nögler, T.F., 2002. Measurement of calcium isotopes ($\delta^{44}\text{Ca}$) using a multicollector TIMS technique. *Int. J. Mass Spectrom.* 220, 385–397.
- Hezel, D.C., Russell, S.S., Ross, A.J., Kearsley, A.T., 2008. Modal abundances of CAIs: Implications for bulk chondrite element abundances and fractionations. *Meteorit. Planet. Sci.* 43, 1879–1894.
- Hin, R.C., Coath, C.D., Carter, P.J., Nimmo, F., Lai, Y.-J., Pogge von Strandmann, P.A., Willbold, M., Leinhardt, Z.M., Walter, M.J., Elliott, T., 2017. Magnesium isotope evidence that accretional vapour loss shapes planetary compositions. *Nature* 549, 511–515.
- Hoare, L., Klaver, M., Saji, N.S., Gillies, J., Parkinson, L.J., Lissenberg, C.J., Millet, M.-A., 2020. Melt chemistry and redox conditions control titanium isotope fractionation during magmatic differentiation. *Geochim. Cosmochim. Acta* 282, 38–54.
- Hoare, L., Klaver, M., Muir, D.D., Klemme, S., Barling, J., Parkinson, L.J., Lissenberg, C.J., Millet, M.-A., 2022. Empirical and experimental constraints on Fe-Ti oxide-melt titanium isotope fractionation factors. *Geochim. Cosmochim. Acta* 326, 253–272.
- Johnson, A.C., Aarons, S.M., Dauphas, N., Nie, N.X., Zeng, H., Helz, R.T., Romaniello, S. J., Anbar, A.D., 2019. Titanium isotopic fractionation in Kilauaea Iki lava lake driven by oxide crystallization. *Geochim. Cosmochim. Acta* 264, 180–190.
- Klaver, M., Ionov, D.A., Takazawa, E., Elliott, T., 2020. The non-chondritic Ni isotope composition of Earth's mantle. *Geochim. Cosmochim. Acta* 268, 405–421.
- Kommischer, S., Fonseca, R.O., Kurzweil, F., Thiemens, M., Munker, C., Sprung, P., 2020. Unravelling lunar mantle source processes via the Ti isotope composition of lunar basalts. *Geochim. Perspect. Lett.* 13, 13–18.
- Leitzke, F., Fonseca, R., Göttlicher, J., Steininger, R., Jahn, S., Prescher, C., Lagos, M., 2018. Ti K-edge XANES study on the coordination number and oxidation state of Titanium in pyroxene, olivine, armalcolite, ilmenite, and silicate glass during mare basalt petrogenesis. *Contrib. Mineral. Petrol.* 173, 1–17.
- Leya, I., Schönbächler, M., Wiechert, U., Krähenbühl, U., Halliday, A.N., 2008. Titanium isotopes and the radial heterogeneity of the solar system. *Earth Planet. Sci. Lett.* 266, 233–244.
- Leya, I., Schönbächler, M., Krähenbühl, U., Halliday, A.N., 2009. New titanium isotope data for Allende and Efremovka CAIs. *Astrophys. J.* 702, 1118–1126.
- Li, J., Tang, S., Zhu, X., Ma, J., Zhao, X., 2022. Titanium isotope analysis of igneous reference materials using a double-spike MC-ICP-MS method. *Acta Geol. Sin.* 96, 517–524.
- Mandl, M.B., 2019. **Titanium isotope fractionation on the Earth and Moon: Constraints on magmatic processes and Moon formation.** Doctoral dissertation (No. 25553), ETH Zurich, Switzerland.
- Mezger, K., Schönbächler, M., Bouvier, A., 2020. Accretion of the Earth - Missing components? *Space Sci. Rev.* 216, 27.
- Millet, M.-A., Dauphas, N., 2014. Ultra-precise titanium stable isotope measurements by double-spike high resolution MC-ICP-MS. *J. Anal. at. Spectrom.* 29, 1444–1458.
- Millet, M.-A., Dauphas, N., Greber, N.D., Burton, K.W., Dale, C.W., Debret, B., Macpherson, C.G., Nowell, G.M., Williams, H.M., 2016. Titanium stable isotope investigation of magmatic processes on the Earth and Moon. *Earth Planet. Sci. Lett.* 449, 197–205.
- Moynier, F., Deng, Z., Lanteri, A., Martins, R., Chaussidon, M., Savage, P., Siebert, J., 2020. Metal-silicate silicon isotopic fractionation and the composition of the bulk Earth. *Earth Planet. Sci. Lett.* 549, 116468.
- Niederer, F., Papanastassiou, D., Wasserburg, G., 1985. Absolute isotopic abundances of Ti in meteorites. *Geochim. Cosmochim. Acta* 49, 835–851.
- Nielsen, S., Bekaert, D., Magna, T., Mezger, K., Auro, M., 2020. The vanadium isotope composition of Mars: Implications for planetary differentiation in the early solar system. *Geochim. Perspect. Lett.* 15, 35–39.
- Rüfenacht, M., Morino, P., Lai, Y.J., Fehr, M.A., Haba, M.K., Schönbächler, M., 2023. Genetic relationships of solar system bodies based on their nucleosynthetic Ti isotope compositions and sub-structures of the solar protoplanetary disk. *Geochim. Cosmochim. Acta* 355, 110–125.
- Rzehak, L.J., Kommischer, S., Kurzweil, F., Sprung, P., Leitzke, F.P., Fonseca, R.O., 2021. The redox dependence of titanium isotope fractionation in synthetic Ti-rich lunar melts. *Contrib. Mineral. Petrol.* 176, 1–16.
- Rzehak, L.J., Kommischer, S., Hoare, L., Kurzweil, F., Sprung, P., Leitzke, F.P., Fonseca, R.O., 2022. Redox-dependent Ti stable isotope fractionation on the Moon: implications for current lunar magma ocean models. *Contrib. Mineral. Petrol.* 177, 81.
- Saji, N.S., Larsen, K., Wielandt, D., Schiller, M., Costa, M.M., Whitehouse, M.J., Rosing, M.T., Bizzarro, M., 2018. Hadean geodynamics inferred from time-varying $^{142}\text{Nd}/^{144}\text{Nd}$ in the early Earth rock record. *Geochem. Persp. Lett.* 7, 43–48.
- Schönbächler, M., Carlson, R.W., Horan, M.F., Mock, T.D., Hauri, E.H., 2010. Heterogeneous accretion and the moderately volatile element budget of Earth. *Science* 328, 884–887.
- Schönberg, R., Zink, S., Staubwasser, M., von Blanckenburg, F., 2008. The stable Cr isotope inventory of solid Earth reservoirs determined by double spike MC-ICP-MS. *Chem. Geol.* 249, 294–306.
- Shollenberger, Q.R., Jordan, M.K., McCain, K.A., Ebert, S., Bischoff, A., Kleine, T., Young, E.D., 2022. Titanium isotope systematics of refractory inclusions: Echoes of molecular cloud heterogeneity. *Geochim. Cosmochim. Acta* 324, 44–65.
- Siebert, C., Nögler, T.F., Kramers, J.D., 2001. Determination of molybdenum isotope fractionation by double-spike multicollector inductively coupled plasma mass spectrometry. *Geochim. Geophys. Geosyst.* 2.
- Simon, J., Jordan, M., Tappa, M., Schauble, E., Kohl, I., Young, E., 2017. Calcium and titanium isotope fractionation in refractory inclusions: Tracers of condensation and inheritance in the early solar protoplanetary disk. *Earth Planet. Sci. Lett.* 472, 277–288.
- Simon, S.B., Sutton, S.R., Grossman, L., 2016. The valence and coordination of titanium in ordinary and enstatite chondrites. *Geochim. Cosmochim. Acta* 189, 377–390.
- Sossi, P.A., Eggins, S.M., Nesbitt, R.W., Nebel, O., Hergt, J.M., Campbell, I.H., O'Neill, H. S.C., Van Kranendonk, M., Davies, D.R., 2016. Petrogenesis and geochemistry of Archean komatiites. *J. Petrol.* 57, 147–184.
- Steenstra, E., Seegers, A., Putter, R., Berndt, J., Klemme, S., Matveev, S., Bullock, E., Van Westrenen, W., 2020. Metal-silicate partitioning systematics of siderophile elements at reducing conditions: A new experimental database. *Icarus* 335, 113391.
- Storck, J.-C., Greber, N.D., Duarte, J.F.V., Lanari, P., Tiepolo, M., Pettke, T., 2023. Molybdenum and titanium isotopic signatures of arc-derived cumulates. *Chem. Geol.* 617, 121260.
- Sutton, S., Goodrich, C., Wirick, S., 2017. Titanium, vanadium and chromium valences in silicates of ungrouped achondrite NWA 7325 and ureilite Y-791538 record highly-reduced origins. *Geochim. Cosmochim. Acta* 204, 313–330.
- Torrano, Z.A., Brennecke, G.A., Williams, C.D., Romaniello, S.J., Rai, V.K., Hines, R.R., Wadhwa, M., 2019. Titanium isotope signatures of calcium-aluminum-rich inclusions from CV and CK chondrites: Implications for early Solar System reservoirs and mixing. *Geochim. Cosmochim. Acta* 263, 13–30.
- Trinquier, A., Elliott, T., Ulfbeck, D., Coath, C., Krot, A.N., Bizzarro, M., 2009. Origin of nucleosynthetic isotope heterogeneity in the solar protoplanetary disk. *Science* 324, 374–376.
- Tusch, J., Sprung, P., Van de Löcht, J., Hoffmann, J., Boyd, A., Rosing, M., Munker, C., 2019. Uniform ^{182}W isotope compositions in Eoarchean rocks from the Isua region, SW Greenland: The role of early silicate differentiation and missing late veneer. *Geochim. Cosmochim. Acta* 257, 284–310.
- Wang, W., Huang, S., Huang, F., Zhao, X., Wu, Z., 2020. Equilibrium inter-mineral titanium isotope fractionation: Implication for high-temperature titanium isotope geochemistry. *Geochim. Cosmochim. Acta* 269, 540–553.
- Williams, N.H., Fehr, M.A., Parkinson, L.J., Mandl, M.B., Schönbächler, M., 2021. Titanium isotope fractionation in solar system materials. *Chem. Geol.* 568, 120009.
- Wlotzka, F., 2005. Cr spinel and chromite as petrogenetic indicators in ordinary chondrites: Equilibration temperatures of petrologic types 3.7 to 6. *Meteorit. Planet. Sci.* 40, 1673–1702.
- Wood, B.J., Kiseeva, E.S., 2015. Trace element partitioning into sulfide: How lithophile elements become chalcophile and vice versa. *Am. Mineral.* 100, 2371–2379.
- Wood, B.J., Smythe, D.J., Harrison, T., 2019. The condensation temperatures of the elements: A reappraisal. *Am. Mineral.* 104, 844–856.
- Zhang, J., Dauphas, N., Davis, A.M., Pourmand, A., 2011. A new method for MC-ICPMS measurement of titanium isotopic composition: Identification of correlated isotope anomalies in meteorites. *J. Anal. at. Spectrom.* 26, 2197–2205.
- Zhang, J., Dauphas, N., Davis, A.M., Leya, I., Fedkin, A., 2012. The proto-Earth as a significant source of lunar material. *Nat. Geosc.* 5, 251–255.
- Zhao, X., Tang, S., Li, J., Wang, H., Helz, R., Marsh, B., Zhu, X., Zhang, H., 2020. Titanium isotopic fractionation during magmatic differentiation. *Contrib. Mineral. Petrol.* 175, 1–16.
- Zhu, K., Hui, H., Klaver, M., Li, S.J., Chen, L., Hsu, W., 2023. Calcium isotope evolution during differentiation of Vesta and calcium isotopic heterogeneities in the inner solar system. *Geophys. Res. Lett.* 50, e2022GL102179.